

Kimberlitic chlorites from Sierra Leone, West Africa: unusual chemistries and structural polytypes

LINDA A. TOMPKINS¹

*Geology Department, University of Massachusetts
Amherst, Massachusetts 01003*

S. W. BAILEY

*Department of Geology and Geophysics
University of Wisconsin, Madison, Wisconsin 53706*

AND STEPHEN E. HAGGERTY

*Geology Department, University of Massachusetts
Amherst, Massachusetts 01003*

Abstract

Chlorites occur as ovoid discrete nodules (1–4 cm), as anhedral macrocrysts (0.20 mm) and euhedral crystals (0.05 mm) in kimberlite, and as cleavage replacement products of high Fe (reversely pleochroic), low Ti + Cr phlogopites. The nodules are severely deformed and four textural groups are recognized (fibrous, platy, tectonized, multiple cleavage) that consist of intergrown chlorites and vermiculites of variable compositions. Major chemical types in the nodules are classified as high Fe (25 wt.%), intermediate Fe (15 wt.%), and low Fe (8 wt.%) varieties with a subgroup consisting of low Fe and high K (0.8–2.3 wt.% K₂O). The chlorites have high SiO₂ (46.6 wt.% max) and MgO (28 wt.% max), and low Al₂O₃ (8–12 wt.%) contents. High Fe³⁺ and later alteration result in vacancies (corroborated by electron densities) in the interlayer sheet. The chlorites and vermiculites are dominantly of the rare Ia structural type, intergrown with more typical IIb chlorite in some specimens. Two-layer “s” and “t” stacking sequences identified in Ia chlorites and vermiculites suggest alteration from parent 1M and 2M₁ phlogopites, respectively. Chloritization of peridotitic phlogopite nodules and macrocrysts took place at relatively low P–T conditions concurrent with, or followed by crystallization of primary magmatic chlorite in the kimberlite groundmass.

Introduction

Chlorite is a common constituent of many rock types and a characteristic component of low grade greenschist facies metamorphism. It is, however, stable over a range of temperature, pressure, and volatile conditions (Albee, 1962). Primary igneous chlorite occurs in some diabases (Lehmann, 1965) and Fawcett (1965) reports chlorite in residual liquids from basalts in Mull. Quenched chlorite is noted by Schreyer and Yoder (1964) in experiments at 5 and 10 kbar at temperatures above the cordierite solidus in the system Mg-cordierite–H₂O. Diamond inclusion studies support the notion of hydrous phyllosilicates in

the upper mantle, and phlogopite (Prinz et al., 1975; Sobolev, 1977), biotite (Giardini et al., 1974), and type Ib chlorite (Mitchell and Giardini, 1977) have been reported. Nixon and Kreston (1973) describe green kimberlitic chlorite and phlogopite cored by chlorite in the Khabes dike, Lesotho. A green pleochroic chlorite occurs along the outer three meters of a kimberlite from the De Beers Mine (Ferguson et al., 1973). These may be late-stage alteration products of phlogopite associated with, or resulting from fluidization and kimberlite emplacement (Kreston, 1973). McGetchin et al. (1973) have characterized three pleochroic types of chlorites resulting from variations in Cr₂O₃ content from the Moses Rock kimberlite and the Cane Valley carbonatite dikes, Utah. Diopsidic pyroxenes from spinel lherzolite are considered to be the precursors to these chlorites via reactions with a volatile-rich fluid phase during kimberlite-carbonatite as-

¹ Present address: B. P. Minerals, 75 Rua Martin Ferreira, Boto Fogo, Rio de Janeiro, Brazil. Reprint requests to S. E. Haggerty.

cent. Chlorite replacement of phlogopite along cleavage planes is also described from the Mir pipe in Siberia (Frantsesson, 1970), and this appears to be directly associated with carbonatitic activity in the pipe.

Chlorite was first recognized as a constituent of the Koidu kimberlite complex in Sierra Leone by Grantham and Allen (1960), but few details are provided. Systematic sampling of the complex (Tompkins, 1983; Tompkins and Haggerty, 1983a,b) now shows that chlorite is abundant and is present in three modes: as large (up to 4 cm) discrete megacrystic nodules, as a primary crystalline component of the kimberlite, and as a replacement product of phlogopite. Chlorites most similar to these are reported from only one other kimberlite locality, the Mbujimayi complex in Zaire (Fieremans and Ottenburgs, 1979). The analytical data, however, are not directly applicable because large concentrations of quartz are present in bulk chemical analyses. The present study was undertaken to characterize the Koidu chlorites, compositionally and structurally, in an attempt to define more accurately their genesis and petrological affinities, and to establish whether chlorite is a viable mineral host for volatiles in the upper mantle.

Geological setting

The Cretaceous–Jurassic kimberlite field in the Leo uplift of eastern Sierra Leone is comprised of three kimberlite pipes, a ring-dike structure, and multiple sets of *en-echelon* kimberlite dikes intruded into Archean age granitic rocks (Hall, 1970). This district forms part of a larger kimberlite province that includes other bodies in Liberia, Guinea, Mali, and the Ivory Coast (Bardet, 1974). The pipes at Koidu are multiple intrusions and several facies of kimberlite are recognized (Tompkins and Haggerty, 1983a,b). Kimberlites at Pipe 1 are typically coarse grained and brecciated, whereas those at Pipe 2 are finer grained and have carbonatitic affinities based on major and minor element bulk chemistries (Tompkins, 1983). The dikes are massive and distinctly basaltic in appearance. Chlorite nodules have thus far been recognized only at Pipe 2. Primary groundmass chlorite, and chlorite replacement of phlogopite is best developed in the dikes and is less prevalent in the diatreme facies. All kimberlite facies are diamond-bearing and the mantle-derived nodule suite is composed of eclogites and discrete megacrysts of Mg-ilmenite, sub-calcic clinopyroxene, and pyrope-rich garnet.

Analytical procedures

Terminology

Nodule is used in the sense generally applied to polymineralic xenoliths hosted in kimberlite, and *megacrysts* are large (usually >2 cm) discrete nodules of a single mineral. Because of the genetic implications implied by *phenocrysts* and *xenocrysts* these terms are only used in specific instances and the term *macrocryst* is employed where there are uncertainties in origin. *Primary*

igneous is used for mineral melt derivatives whereas *replacement* (or *secondary*) implies a solid state reaction derived from deuteric processes or post-consolidation activity.

Optical techniques

Chlorite nodules were examined and classified in hand specimen and under a binocular microscope. Thick polished mounts were found to be more useful than polished-thin-sections in revealing subtleties in cross fiber relations. Transmitted and reflected light microscopy was used for the study of kimberlites.

Chemistry

Chemical analyses of mineral assemblages and intergrowths were determined using an ETEC automated electron microprobe at the University of Massachusetts. Accelerating voltage was 15 kV, with a beam diameter of 5 μm and a specimen current of 0.03 nA. Matrix correction factors are those of Bence and Albee (1968) and Albee and Ray (1970). Synthetic (s) and natural (n) standards used are as followed: pyrope garnet, P-130 (n) for Fe, Al; Mn-ilmenite (n) for Ti, Mn; Fe_{93} , P-130 (n) for Mg; kyanite (n) for Si; chromite, Cr-cats (s) for Cr; jadeite, Jd-35 (s) for Na, Ca; sanidine (n) for K.

Iron was determined by microbeam analysis but ferrous iron was determined on discrete nodules by wet chemical analyses following the Wilson cold digestion procedure as outlined by Maxwell (1968). Triplicate analyses were compared with two standards, BCR-1 and Knippa-1. These standards are routinely used in XRF analyses at the University of Massachusetts; the USGS analyses are given in Flanagan (1976). Deviations of the standards from the mean were no greater than ± 0.10 wt.%. The wet chemical ferrous iron determinations of chlorite nodules represent bulk compositions. Ferrous and ferric iron contents were calculated from weighted averages based on chlorite modal analyses in those nodules having more than one compositional type.

X-ray crystallography

Four chlorite nodules were studied by X-ray powder and single crystal techniques. Samples CHK-1 and CHK-6 were selected as representative of the fibrous chlorites and CHK-2 and CHK-13 of the platy and tectonized chlorites. Gandolfi patterns were taken of individual fibers and plates as well as Debye-Scherrer patterns using crushed material in capillary tubes with $\text{FeK}\alpha$ radiation. From three to six individual fibers or plates from each nodule were also studied by precession and Weissenberg methods to determine the precise stacking sequence of layers. The 00l intensities for crystals from samples CHK-1 and CHK-2 were measured on a single crystal diffractometer, corrected for Lp and absorption factors, and used to calculate one-dimensional electron density maps.

Chlorite occurrence and mineral associations

Discrete chlorite nodules

The discrete chlorite nodules (Fig. 1) are similar to other members of the megacryst suite (pyroxene, garnet, ilmenite) at Koidu with respect to size (1–4 cm) and their oval and abraided appearance. In hand specimen the nodules are dark forest green in color with veinlets of

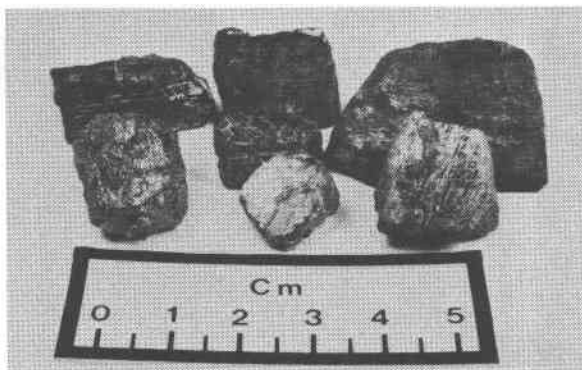


Fig. 1. A representative collection of the four discrete chlorite nodule groups identified at Koidu. Textural types from left to right are: back row, all group F; front row, groups T, P, C; center, group F.

mustard yellow serpentine. Their habit is variable and four major groups are recognized. Group F (*fibrous*) chlorites are cohesive and consist of nodules with a filiform to bladed habit. Group P (*platy*) are characterized by chlorites that form books or plates typical of phyllosilicate minerals. Group T (*tectonized*) are characterized by single distinct parting planes. Textures are platy to fibrous and many nodules are bent or multiply contorted. Group C (*multiple cleavage*) are composed of nodules with two distinct parting directions. Examples of a selection of these groups are illustrated in Figure 2a–f. Anastomosing networks of crosscutting fibers (Fig. 2a–d) are present in some nodules and these crossfibers form distinct subparallel groups. Typically, one set of crossfibers is observed but two sets may also be present (Fig. 2d). Compositionally, these fine cross-fibers are usually similar to the host phase. In Figure 2d, however, hardness, reflectivity, and chemical differences are evident and the harder and darker cross-fibers are selectively replaced by serpentine (highly reflective phase). In Figure 2e–f the flame-like structures are two compositionally distinct chlorites intergrown along the same cleavage planes. Kink banding perpendicular to the cleavage disrupts this parallelism giving the appearance of cross-cutting fibers. These textures are interpreted to result from deformation and rehealing along brittle fracture planes and are very similar to those described by Boyd and Nixon (1978) for lherzolitic phlogopites from kimberlites in South Africa.

Macrocrysts and groundmass chlorite

When calcite is the major matrix mineral, groundmass chlorite is found with only minor modal amounts of Ti, Cr-rich phlogopite. In those kimberlites where matrix serpentine is predominant, however, groundmass Ti, Cr-rich phlogopite is abundant and chlorite is sparse or absent. Large (0.25–0.5 cm) chlorites are anhedral and xenocrystic in appearance but finer grained groundmass chlorites are present as perfect euhedral platelets (Fig. 3a)

averaging ≈ 0.05 mm in cross-section. They occur either as disseminated crystals in the carbonatitic-kimberlite groundmass or as aggregate platelets (Fig. 3b) in carbonate rich pockets of less carbonated kimberlite. In some cases the platelets are optically zoned (Fig. 3a). These chlorites as well as the others are strongly pleochroic in deep blue-green with abnormal blue interference colors and a small negative $2V$ ($\approx 15^\circ$). Occasional decomposition of macrocrystic chlorite results in the formation of admixtures of goethite + hematite + complex intergrowths of finely disseminated calcite and silicate minerals (Fig. 3c). Expansion of the sheet silicate and swelling and distortion of the chlorite takes place.

Replacement chlorite

Reversely (R) pleochroic phlogopites ($\alpha > \gamma$, where $\alpha = \tan$, and $\gamma = \text{colorless}$) form cores to normally (N) pleochroic phlogopites ($\alpha < \gamma$, where $\alpha = \text{colorless}$ and $\gamma = \tan$ in color). The early phlogopites (R) are preferentially replaced by chlorite along cleavage planes (Fig. 3d). The phlogopites are consistently >0.1 mm in longest dimension, and phlogopites (R) similar to these have been described from a number of kimberlites in South Africa (Farmer and Boettcher, 1981).

Mineral chemistry

Representative averages of electron microbeam analyses of the Koidu chlorites are listed in Tables 1–3. Previously published kimberlitic chlorite compositions are also presented and have been recalculated based on a theoretical 28 oxygen formula cell. In most of the Koidu chlorites studied, two, three, or in some cases four distinct compositions were determined. Some of the components are evident in the photomicrographs in Figure 2 but others are not illustrated and are on a much finer scale.

Major elements

The unusual chemistry of the chlorites is distinguished by their low Al_2O_3 (8–12 wt.%), high SiO_2 (28.97–41.65 wt.%), and MgO (19.0–28.0 wt.%) values coupled with high Fe (up to 29.5 wt.% as FeO).

Nodules (CHK-1, 2, and 3) with two compositional types in groups F, D, and T (Table 1) have hosts with low FeO_T (≈ 7 wt.%), high SiO_2 (≈ 41 wt.%), and Al_2O_3 averaging 11.5 wt.%. This compositional type is referred to as low iron chlorite. By contrast, the high iron chlorites average 21.5 wt.% FeO_T , are lower in SiO_2 (31.7 wt.%), and lower in Al_2O_3 (8.6 wt.%). The average MgO contents in both the high and low iron chlorites is 26 wt.%.

Nodule CHK-7 (group F) has three compositional types (Table 2), a high iron chlorite host (the inverse of CHK-1, 2, and 3), a low Fe chlorite (8.7 wt.% FeO_T), and a chlorite of intermediate FeO_T (13.1 wt.%) content. Aluminum and SiO_2 vary sympathetically and MgO ranges from 24–28 wt.%.

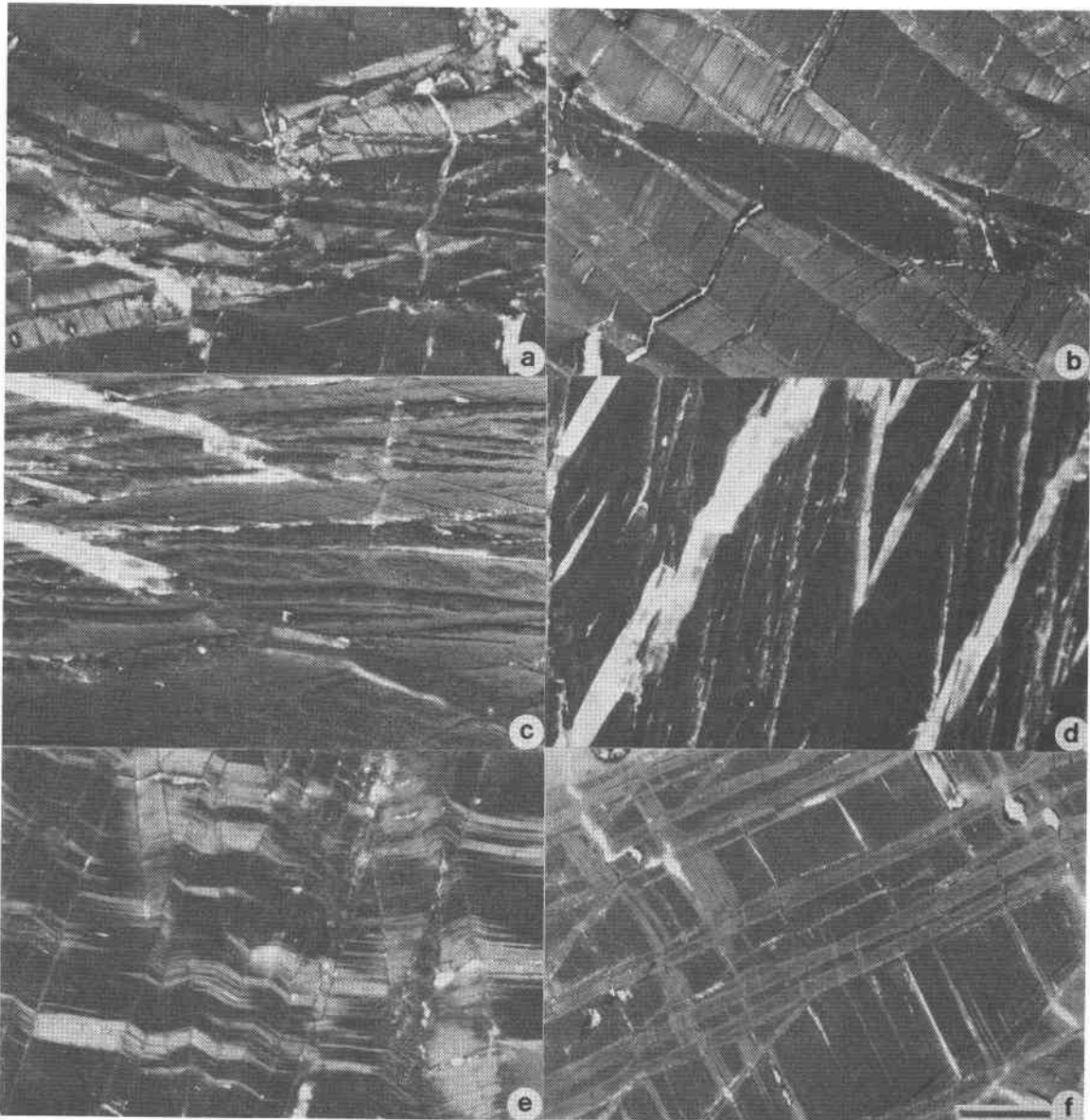


Fig. 2. Reflected light photomicrographs of discrete nodules in polished sections illustrating the variety of observed textural forms. a) CHK-1. Anastomosing network of cross-cutting fibers (dark phase). Both the host chlorite and cross-fiber chlorite are low Fe chlorites (analysis A, Table 1). b) A coarser cross-fiber from CHK-1. c) CHK-7. The host phase is the lighter and softer phase. This phase is high in Fe (analysis C, Table 2). Cross-fibers are low in Fe (analyses A and B, Table 2), and are easily distinguished in this nodule by its greater hardness and lower reflectivity. The highly reflective phase is serpentine replacing the low Fe cross-fibers. d) CHK-7. This photomicrograph is similar to C except that the cross-fibers are completely replaced by serpentine. e) CHK-1. Well formed kink bands run approximately N-S perpendicular to the cleavage giving the appearance of cross-cutting fibers. The lighter flame-like phase is the high Fe chlorite (analysis B, Table 1), the darker flame-like phase is the low Fe chlorite (analysis A, Table 1). f) CHK-1. Same as e, except that fine cross-cutting fibers are visible. Scale bar = 0.2 mm.

Nodule CHK-13 (group T) has four compositional components (Table 2) of which three are approximately in equal proportions. Here again, low and high iron chlorites are present, but in addition there are two intermediate iron chlorites having 10 and 15 wt.% FeO_T .

Compositions of five additional nodules (CHK-4, 1B,

3B, 4B, and 9) are given in Table 2, representing groups F, T, and C. These nodules have not been characterized in the same detail but the major compositional host phases are high, low, or intermediate iron chlorites, similar in major element compositions to those described above. The replacement chlorites (Fig. 3d) in phlogopite

Table 1. Compositions of discrete chlorite nodules.

X	CHK-1 (F)			CHK-2 (P)			CHK-3 (T)				CHK-6 (F)		
	A	B	BULK	A	B	BULK	A	B	C	BULK	A	B	BULK
SiO ₂	40.98	33.51	39.11	30.51	41.44	35.98	31.09	41.21	41.29	40.20	41.65	41.42	41.54
TiO ₂	0.17	0.15	0.17	0.14	0.18	0.16	0.16	0.20	0.21	0.20	0.22	0.22	0.22
Al ₂ O ₃	10.89	9.16	10.46	8.33	11.71	10.02	8.18	11.83	11.56	11.46	11.89	11.72	11.81
Cr ₂ O ₃	0.12	0.09	0.11	0.07	0.08	0.08	0.11	0.12	0.12	0.12	0.16	0.16	0.16
Fe ₂ O ₃	-----	-----	10.81 ⁺	-----	-----	11.72 ⁺	-----	-----	-----	6.39 ⁺	-----	-----	4.07 ⁺
FeO	7.83	26.37	2.74	19.01	7.84	2.88	18.83	8.00	8.00	3.33	6.66	6.97	3.16
MgO	25.84	21.91	24.86	26.86	25.88	26.37	27.80	26.73	26.30	26.83	26.21	25.78	26.00
MnO	0.02	0.04	0.03	0.09	0.07	0.08	0.08	0.03	0.20	0.04	0.01	0.00	0.01
CaO	0.15	0.22	0.17	0.24	0.18	0.21	0.25	0.09	0.10	0.11	0.00	0.09	0.05
Na ₂ O	0.01	0.03	0.02	0.02	0.01	0.02	0.00	0.00	0.02	0.00	0.00	0.02	0.01
K ₂ O	0.01	0.00	0.01	0.08	0.47	0.28	0.06	0.26	0.79	0.25	0.15	1.45	0.80
Total	86.02	91.48	88.49	85.35	87.86	87.80	86.56	88.47	88.59	88.93	86.95	87.83	87.83
Cations to 28 Oxygens *													
Si	7.810	6.772	7.355	6.454	7.754	6.927	6.468	7.662	7.704	7.435	7.797	7.765	7.700
Ti	0.025	0.023	0.024	0.023	0.026	0.023	0.025	0.028	0.029	0.028	0.032	0.032	0.031
Al ^T	2.448	2.182	2.319	2.077	2.582	2.273	2.007	2.592	2.543	2.498	2.623	2.589	2.580
Cr	0.018	0.015	0.016	0.011	0.012	0.013	0.018	0.018	0.018	0.018	0.023	0.024	0.023
Fe ³⁺	-----	-----	1.530	-----	-----	1.698	-----	-----	-----	0.889	-----	-----	0.568
Fe ²⁺	1.249	4.456	0.431	3.363	1.227	0.464	3.277	1.243	1.248	0.514	1.043	1.093	0.490
Mg	7.345	6.599	6.969	8.468	7.218	7.567	8.621	7.408	7.314	7.396	7.313	7.203	7.183
Mn	0.003	0.007	0.005	0.017	0.011	0.013	0.014	0.004	0.031	0.007	0.001	0.000	0.001
Ca	0.030	0.047	0.034	0.055	0.036	0.043	0.056	0.018	0.020	0.022	0.000	0.018	0.010
Na	0.005	0.012	0.007	0.008	0.007	0.007	0.000	0.000	0.007	0.000	0.000	0.007	0.003
K	0.002	0.000	0.002	0.022	0.112	0.068	0.016	0.061	0.188	0.059	0.036	0.347	0.189
Total	18.935	20.113	18.692	20.498	18.985	19.096	20.502	19.034	19.102	18.866	18.868	19.078	18.778
#	7	6		7	7		3	4	4		4	8	
%	75	25		50	50		10	88	2		50	50	
Tet. Al	0.190	1.228	0.645	1.546	0.246	1.073	1.532	0.338	0.296	0.565	0.203	0.235	0.300
Oct. Al	2.258	0.954	1.674	0.531	2.336	1.200	0.475	2.254	2.247	1.933	2.420	2.354	2.280

(X) sample number and textural type.

* Based on the unit cell assuming theoretical O(OH) content

+ Based on the difference obtained by wet chemical analysis for FeO

Number of analyses averaged together

% Estimated modal percent used in bulk analysis computation

as well as the groundmass chlorites (Fig. 3a-b, Table 3) are high Fe compositional types.

Considering the bulk compositions of the entire group, the three chemical chlorite types may now be defined as low (7-10 wt.% FeO_T), intermediate (12-14 wt.% FeO_T), and high (17-20 wt.% iron varieties).

In order to maintain charge balance, a large amount of ferric iron is required for the higher Fe chlorite varieties in the absence of major concentrations of other trivalent cations. Even though the low Fe varieties contain higher octahedral Al, considerable Fe³⁺ or octahedral vacancies are necessary assuming a formula fit to theoretical chlorite. The low Fe varieties, however, yield a reasonable cation total to a theoretical vermiculite formula of 22 oxygens and these phases may indeed be vermiculite or interstratified vermiculite/phlogopite (i.e., CHK-13, analysis D) or vermiculite/chlorite. Because of probable multicomponent complexities in these phases the theoretical 28 oxygens is used. This is a reasonable assumption for most chlorites (Foster, 1962) but it is possible that some oxygen has replaced (OH); this increases the cation total but decreases tetrahedral Al which in many cases is already fairly low. Variations in Al, Fe²⁺, and Mg are shown in Figure 4 and are compared to chlorites from other kimberlites. A well-defined trend is apparent for the Koidu and Mir chlorites and for some of the Utah

samples; a few of the latter are enriched in Mg and are slightly removed from the arcuate trend displayed by the remaining groups.

Minor elements

The Koidu chlorites have minor concentrations of MnO (0.09 wt.% max), Cr₂O₃ (0.51 wt.% max), and TiO₂ (0.14-0.43 wt.%). There is a tight cluster of the latter two oxides around 0.1 wt.% Cr₂O₃ and 0.2 wt.% TiO₂ (Fig. 5). The few anomalously high contents are associated with groundmass chlorites and one of the chlorite nodules. The minor element concentration of the Koidu chlorites are markedly different from those of the Utah specimens, which are high chromium chlorites (0.23-3.90 wt.% Cr₂O₃). The chlorite from the Mir pipe, however is similar to the Koidu samples having 0.26 wt.% Cr₂O₃, and 0.32 wt.% TiO₂.

Na, K, and Ca

Sodium contents are minimal in all kimberlitic chlorites with a maximum of 0.07 wt.% Na₂O for those at Koidu to 0.03 wt.% Na₂O for the Utah and Siberia samples. Potassium, however, is present in concentrations of up to 2.31 wt.% K₂O, and CaO contents up to 0.25 wt.% were detected for Koidu. The modal proportions of the high

Table 2. Compositions of discrete chlorite nodules.

X	CHK-7 (F)				CHK-13 (T)					CHK-4 (C)	CHK-1B (F)	CHK-3B (T)	CHK-4B (C)	CHK-9 (F)
	A	B	C	BULK	A	B	C	D	BULK					
SiO ₂	41.00	37.73	29.64	32.27	28.97	34.93	41.35	39.20	35.83	34.62	35.11	32.53	32.12	39.12
TiO ₂	0.19	0.19	0.14	0.16	0.22	0.20	0.20	0.21	0.21	0.15	0.20	0.35	0.20	0.21
Al ₂ O ₃	12.02	10.91	8.12	9.18	8.60	9.95	11.56	11.16	10.27	10.17	10.96	9.42	9.32	10.19
Cr ₂ O ₃	0.15	0.13	0.08	0.10	0.06	0.09	0.08	0.09	0.08	0.11	0.12	0.05	0.13	0.07
Fe ₂ O ₃	-----	-----	-----	14.65 ⁺	-----	-----	-----	-----	6.95 ⁺	14.89 ⁺	7.33 ⁺	15.57 ⁺	17.66 ⁺	3.96
FeO	8.67	13.06	22.31	5.47	29.55	15.44	7.76	10.03	10.38	3.28	4.91	2.90	3.43	4.03
MgO	27.54	27.95	23.79	24.96	19.66	27.51	25.54	24.66	23.42	27.41	29.29	28.07	27.09	25.13
MnO	0.01	0.01	0.06	0.05	0.01	0.01	0.00	0.01	0.01	0.08	0.09	0.06	0.06	0.03
CaO	0.07	0.09	0.14	0.12	0.13	0.09	0.06	0.15	0.12	0.17	0.33	0.13	0.14	0.03
Na ₂ O	0.00	0.00	0.02	0.01	0.04	0.00	0.00	0.03	0.02	0.06	0.16	0.06	0.10	0.03
K ₂ O	0.01	0.02	0.01	0.01	0.01	0.03	0.09	2.31	0.81	0.01	0.25	0.02	0.01	0.16
Total	89.66	90.09	84.31	86.98	87.25	88.25	86.64	87.85	88.10	90.95	88.75	89.16	90.26	82.96
Cations to 28 Oxygens *														
Si	7.548	7.143	6.470	6.472	6.347	6.892	7.812	7.554	7.048	6.534	6.688	6.308	6.217	7.706
Ti	0.027	0.027	0.024	0.024	0.037	0.030	0.028	0.030	0.031	0.022	0.029	0.051	0.029	0.031
Al	2.608	2.434	2.089	2.170	2.222	2.314	2.574	2.535	2.381	2.262	2.461	2.153	2.126	2.366
Cr	0.022	0.019	0.014	0.016	0.010	0.014	0.012	0.014	0.013	0.016	0.018	0.008	0.021	0.011
Fe ³⁺	-----	-----	-----	2.211	-----	-----	-----	-----	1.028	2.115	1.051	2.272	2.573	0.587
Fe ²⁺	1.335	2.068	4.072	0.917	5.418	2.548	1.226	1.616	1.708	0.518	0.782	0.471	0.555	0.664
Mg	7.557	7.888	7.740	7.461	6.425	8.091	7.192	7.083	6.867	7.711	8.317	8.112	7.815	7.378
Mn	0.001	0.001	0.010	0.008	0.002	0.001	0.000	0.001	0.001	0.012	0.015	0.009	0.009	0.005
Ca	0.013	0.018	0.033	0.025	0.030	0.019	0.012	0.031	0.025	0.034	0.068	0.027	0.029	0.006
Na	0.000	0.000	0.008	0.002	0.016	0.000	0.000	0.012	0.007	0.022	0.060	0.022	0.037	0.012
K	0.002	0.005	0.003	0.004	0.003	0.007	0.022	0.567	0.203	0.002	0.062	0.005	0.002	0.040
Total	19.113	19.603	20.463	19.310	20.510	19.916	18.878	19.443	19.312	19.248	19.551	19.438	19.413	18.806
#	5	4	15		10	5	8	5		5	3	8	5	15
%	20	10	70		34	9	23	34						
Tet. Al	0.452	0.857	1.530	1.528	1.653	1.108	0.188	0.446	0.952	1.466	1.312	1.692	1.783	0.294
Oct. Al	2.156	1.577	0.559	0.642	0.569	1.206	2.386	2.089	1.429	0.796	1.149	0.461	0.343	2.072

(X) sample number and textural type.

* Based on the unit cell assuming theoretical O(OH) content.

+ Based on the difference obtained by wet chemical analysis for FeO.

Number of analyses averaged together.

% Estimated modal percent used in bulk analysis computation

K₂O chlorites are 2% (CHK-3, group T, analysis C, Table 1), 50% (CHK-6, group F, analysis B, Table 1), and 34% (CHK-13, group T, analysis D, Table 2). These are all low Fe chlorites. Both K and Ca are considered to be incompatible with the chlorite structure (Pauling, 1930; Foster, 1962). It is likely that the K (+Ca) is present either in an interstratified phlogopite-(chlorite and/or vermiculite) phase or in incompletely replaced phlogopite crystals.

Combined elemental relations

In order to consider all elements on a single two-dimensional plot, the compositional space shown in Figure 6 is useful and is adopted from Robinson et al. (1982). All kimberlitic chlorite analyses are plotted including those from the Cane Valley diatreme, the Moses Rock dikes, and the Mir pipe. Ideal trioctahedral ("Tri") clinocllore is shown and with increasing substitution of Al ideal chlorite compositions plot along the clinocllore-amesite join (Fig. 6). Ideal chlorite compositions with Al substitution less than that of ideal clinocllore plot towards serpentine and away from clinocllore. Data for kimberlitic chlorites from Utah and Siberia lie along this trend. Displacements from this join and towards olivine-spinel (ol-sp) indicate that ferric iron is present. Similarly, chlorites plotting to the right of this join have variable degrees of octahedral vacancies. The Koidu chlorites show an enrichment of Si relative to ideal clinocllore and

two subtle groups are present. One group consists of the high Fe chlorites (i.e., softer lighter phase, Fig. 2c and light flame-like phase Fig. 2e-f) plotting to the left of the clinocllore-serpentine join. When ferric iron is considered, these chlorite compositions move towards the "Tri-Di" octahedral region parallel to the join clinocllore-"Di". The second group is defined by the low Fe and high Si (\pm K₂O) chlorites (i.e., crossfibers, Fig. 2c and the dark phases in Fig. 2e-f). These compositions plot towards talc (vermiculite) with ferric iron having less influence. Compositions are displaced to the right of these data after consideration of Fe³⁺ in the analyses.

Naturally occurring chlorites with octahedral vacancies were summarized by Eggleton and Bailey (1967) and are plotted as a field in Figure 6. Natural dioctahedral chlorites show a range in Si-R³⁺ with Al being the dominant trivalent cation. "Di-Tri" octahedral chlorites show an enrichment of Si relative to ideal compositions and again the trivalent cation is predominantly Al. No naturally occurring "Tri-Di" octahedral chlorites have yet been found (Bailey, 1980). In chlorites, the lower the Si and the higher the tetrahedral Al values, the stronger will be the resulting interlayer bonding (Foster, 1962). Ideally, octahedral R³⁺ cations should equal tetrahedral Al³⁺ cations, but this rarely happens in nature. For the high Fe chlorites, tetrahedral Al is far in excess of octahedral Al (Tables 1-3). In order to maintain charge balance some

Table 3. Compositions of serpentine and other chlorites.

	Serpentine		Groundmass Chlorites				KD-80-5
	CHK-1	CHK-3	KD-80-17-D2A-B				
SiO ₂	42.09	40.90	32.78	33.52	32.94	32.94	31.51
TiO ₂	0.07	0.06	0.19	0.23	0.37	0.19	0.43
Al ₂ O ₃	0.60	0.52	9.66	9.35	9.59	9.28	8.71
Cr ₂ O ₃	0.02	0.00	0.08	0.40	0.04	0.06	0.51
Fe ₂ O ₃	3.87	3.07	18.11	17.27	18.82	17.89	17.85
MgO	38.86	40.87	26.83	26.33	27.03	26.97	27.12
MnO	0.04	0.02	0.08	0.07	0.04	0.07	0.05
CaO	0.11	0.18	0.16	0.12	0.12	0.19	0.12
Na ₂ O	0.01	0.00	0.00	0.00	0.00	0.00	0.04
K ₂ O	0.03	0.02	0.36	0.01	0.16	0.20	0.04
NiO	0.03	0.00	NA	NA	NA	NA	NA
Total	85.73	85.64	88.25	87.30	89.11	87.79	86.38
Cations to 7 oxygens*							
Si	2.007	1.953	6.620	6.786	6.598	6.672	6.523
Ti	0.003	0.002	0.028	0.035	0.056	0.029	0.067
Al	0.034	0.029	2.300	2.233	2.266	2.217	2.124
Cr ³⁺	0.001	0.000	0.013	0.064	0.007	0.010	0.083
Fe ²⁺	0.154	0.123	3.060	2.925	3.154	3.032	3.090
Mg	2.764	2.911	8.081	7.948	8.074	8.146	8.369
Mn	0.001	0.001	0.013	0.011	0.007	0.013	0.009
Ca	0.006	0.009	0.034	0.025	0.026	0.041	0.026
Na	0.001	0.000	0.000	0.000	0.002	0.000	0.015
K	0.002	0.001	0.093	0.003	0.040	0.053	0.010
Ni	0.001	0.000	NA	NA	NA	NA	NA
Total	4.974	5.029	20.242	20.030	20.230	20.213	20.316
#	5	1	3	1	3	1	7
Tet. Al			1.380	1.214	1.402	1.328	1.477
Oct. Al			0.920	1.019	0.864	0.889	0.647
Published data on kimberlitic chlorites							
	3	4	5	6	7	10	20
SiO ₂	32.40	31.90	30.60	36.50	31.60	30.48	34.30
TiO ₂	0.03	0.00	0.03	0.08	0.03	0.32	0.00
Al ₂ O ₃	11.40	12.10	15.90	7.07	14.10	8.42	8.70
Cr ₂ O ₃	3.80	3.90	1.06	0.23	2.40	0.26	0.00
Fe ₂ O ₃	2.90	2.40	4.40	7.70	4.10	7.31	9.20
MgO	35.10	35.00	33.40	34.30	33.90	25.18	40.30
MnO	0.02	0.00	0.02	0.10	0.04	0.06	0.00
CaO	0.00	0.00	0.00	0.00	0.01	3.70	0.50
Na ₂ O	0.00	0.00	0.01	0.03	0.01	0.00	0.00
K ₂ O	0.02	0.00	0.01	0.36	0.00	0.30	0.00
NiO	NA	NA	NA	NA	NA	0.13	NA
Total	85.67	85.30	85.43	86.37	86.19	82.97	93.00
Cations to 28 oxygens*							
Si	6.287	6.203	5.946	7.108	6.078	6.445	6.307
Ti	0.005	0.000	0.005	0.012	0.005	0.051	0.000
Al	2.607	2.773	3.641	1.623	3.265	2.099	1.886
Cr ³⁺	0.583	0.599	0.162	0.035	0.365	0.043	0.000
Fe ²⁺	0.471	0.390	0.714	1.254	0.660	1.164	1.415
Mg	10.153	10.144	9.672	9.955	9.719	7.936	11.045
Mn	0.003	0.000	0.004	0.016	0.007	0.010	0.000
Ca	0.000	0.000	0.000	0.000	0.002	0.839	0.098
Na	0.000	0.000	0.005	0.012	0.005	0.000	0.000
K	0.002	0.000	0.002	0.089	0.000	0.081	0.000
Ni	NA	NA	NA	NA	NA	0.022	NA
Total	20.111	20.109	20.151	20.104	20.106	19.894	20.751
Tet. Al	1.713	1.797	2.054	0.892	1.922	1.555	1.693
Oct. Al	0.894	0.976	1.587	0.731	1.343	0.544	0.193

* Based on the unit cell assuming theoretical O(OH) content.

Number of analyses averaged together.

3,5,7 from carbonatite-kimberlite dikes, Cane Valley diatreme, McGetchin *et al.* (1973)4,6 from kimberlite, Moses Rock dike (sample 1416A), McGetchin *et al.* (1973)

10 from Mir pipe, Siberia, Frantsesson, (1970), table 24.

20 Diamond inclusion. Mitchell and Giardini (1977).

Fe³⁺ must proxy for octahedral Al or some substitution of (OH)⁻ for O²⁻ may take place. There is probably an excess of Fe³⁺ beyond the 1:1 replacement of Al³⁺, and Fe³⁺ will, therefore, replace octahedral divalent cations in a ratio of 2:3. In the low Fe chlorites, octahedral Al is greater than tetrahedral Al and the replacement of R²⁺ cations in the 2:3 ratio is dominated by Al³⁺; ferric iron is the major substituting ion in the high Fe chlorites. In either case, octahedral vacancies are required.

Chlorite structural types

X-ray study shows that the layer-interlayer assemblages are dominantly of the *Ia* type in all four samples examined. This terminology is from Bailey and Brown (1962), in which the symbol *I* means that the directions of stagger of the octahedral sheets in the 2:1 layer and the interlayer are the same, and *a* means that interlayer cations project normal to the layers onto tetrahedral cations in the 2:1 layers above and below (Shirozu and Bailey, 1965). The close approach of interlayer and tetrahedral cations in the *a* position leads to cation-cation repulsion and consequent instability relative to the alternative *b* position. This accounts for the fact that *Ia* chlorites were the least abundant among the 303 chlorite specimens included in a survey of the abundances of structural types in nature by Bailey and Brown (1962). On the other hand, the *Ia* structural type is the only one found to date in vermiculite, where enhanced stability is gained primarily by having relatively few interlayer cations and secondarily by cation order patterns that achieve local charge balance (Shirozu and Bailey, 1966). Interlayer vacancies would enhance the stability of the *Ia* structural type in chlorite also, and it is noteworthy that Hayes (1970) tentatively concluded that *Ia* chlorites found in sedimentary rocks are transitional to vermiculite. This is the case in the Koidu chlorites also, where significant numbers of interlayer vacancies in all of the samples have been inferred from the chemical data of the preceding section and interlayer vacancies have been confirmed in two of the samples (CHK-1, and CHK-2) based on electron density measurements (Fig. 7).

Figure 7 was constructed using 28 00l reflections for each crystal after least-squares refinement of *z*-coordinates, cation multiplicities, and isotropic B values. The electron density in the interlayer sheet at *z/c* = 0° is very low (about 13 e⁻ in CHK-1 and 22 e⁻ in CHK-2) relative to that of the octahedral cation plane in the 2:1 layer at *z/c* = 180° (about 44 e⁻ and 46 e⁻). The densities for the tetrahedral cation plane at *z/c* = 110.9° suggest substitution of 0.1 atoms of tetrahedral Fe³⁺ per formula unit in CHK-1 and 0.2 atoms in CHK-2.

The low interlayer cation electron density and the broad peaks in the map of CHK-1 suggest that this specimen approaches true vermiculite, whereas specimen CHK-2 is slightly more chloritic. This has been confirmed by heating tests. Pieces of specimens CHK-1, CHK-2, CHK-6, and CHK-13 were ground under acetone, prepared as oriented slides, and heated at 600°C in a muffle furnace for one hour. X-ray powder diffractograms obtained in a dry air environment showed that the 14Å spacings of the untreated samples had collapsed completely to 10Å in specimens CHK-1 and CHK-6 and about 60% had collapsed to 10Å in specimens CHK-2 and CHK-13. The complete collapse of specimens CHK-1 and CHK-6 relative to the two other Koidu specimens is in accord with the differences observed in their 00l intensities.

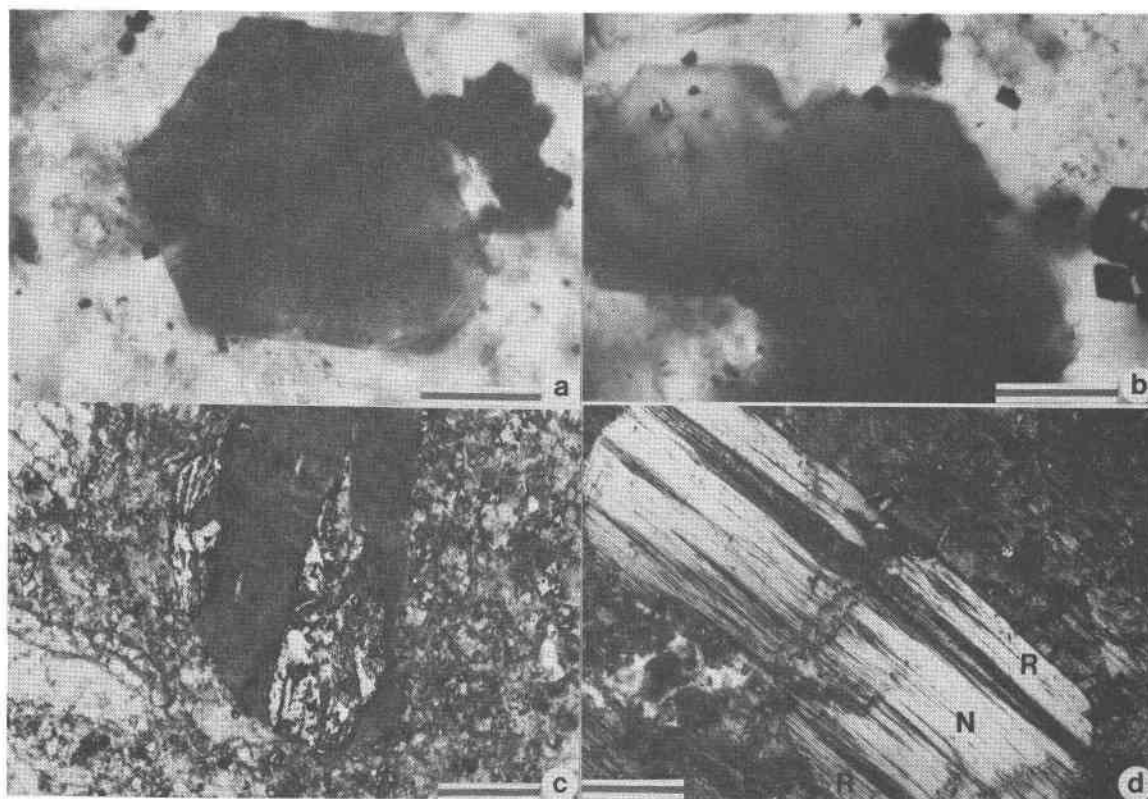


Fig. 3. a) Euhedral groundmass chlorite from section KD-80-5. Microprobe analyses of this grain are given in Table 4. Transmitted light, air objective. b) Stacked chlorite platelets in groundmass kimberlite from section KD-80-5. Transmitted light, air objective. c) Chlorite (center) alteration to goethite and hematite (highly reflective phase), from section KD-80-13. Microprobe analyses are not given. Transmitted and reflected light, air objective. d) Early reversely pleochroic (R) phlogopite rimmed by late stage kimberlitic phlogopite with normal pleochroism (N), from section KD-80-7, area A, grain 3. Dark areas in the core phlogopite are chlorite. Microprobe traverse analyses across this grain are given in Tompkins and Haggerty (1983b). Transmitted light, air objective. Scale bars (a-b = 0.05mm; c-d) = 0.2mm.

ties. Vermiculite samples CHK-1 and CHK-6 have extremely strong 14\AA intensities, which are a consequence of the small amount of scattering power present in the interlayers. The 14\AA peaks in the other two samples are intensified also, but not to the same degree. For example, the $14\text{\AA}/7\text{\AA}$ intensity ratio for the untreated CHK-1 sample is 37.0 and for the CHK-2 sample is 1.8.

Although stacking of adjacent 14\AA structural units is often semi-random in chlorite, this is not the case in the Koidu specimens. The fibrous vermiculite specimens CHK-1 and CHK-6 were found to be the same, for the fibers sampled, and to have the fibers oriented parallel to crystallographic Y . All fibers have a 2-layer structure of the type labeled "s" by Mathieson and Walker (1954), in which there is an L type shift within each 2:1 layer ($-a/3$ parallel to the symmetry plane) and adjacent layers are also shifted by $+b/3$ and $-b/3$ relative to one another. No second phase was found by either powder or single crystal patterns of the CHK-1 and CHK-6 samples for the fibers studied.

Shirozu and Bailey (1966) refined the structure of a 2-layer "s" type vermiculite from Llano County, Texas, and consider the "s" sequence to be the most stable structure for vermiculite. De la Calle et al. (1976) and De la Calle et al. (1978) determined experimentally that the "s" structure occurs only as a result of vermiculitization of phlogopite-1M. The transformation is reversible in the laboratory. They designate the "s" structure as the V_1 type and illustrate identification of different vermiculite structures by means of the diagnostic $02l$ reflections. They point out that the observed diffuseness of these reflections in V_1 indicates a semi-ordered structure having mistakes in the regularity of the $+b/3$ and $-b/3$ shifts, relative to the ideal regular "s" model, such that there is equal probability of a given layer having a $+b/3$ or $-b/3$ shift.

Specimen CHK-2 is platy. One of the four platelets studied by precession photography showed a superposition of Ia and IIb type patterns. The other platelets showed only the Ia single crystal pattern, but abundant

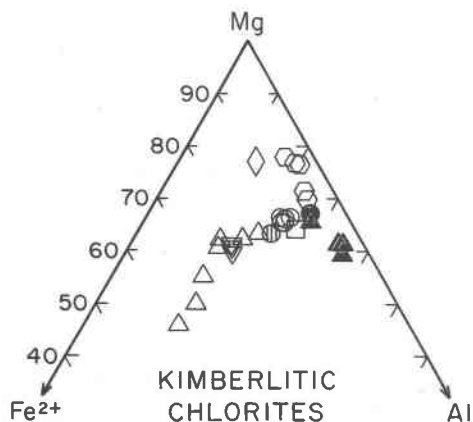


Fig. 4. All chlorite analyses are plotted as a function of Fe^{2+} -Mg-Al. Open circles = low Fe chlorites; Hatched circle = low Fe/phlogopite analysis CHK-13-D, Table 2; Closed circles = low Fe samples not fully characterized; Open apex up triangles = high Fe chlorites; Closed apex up triangles = samples not fully characterized; Open apex down triangles = groundmass chlorites; Open square = Mir pipe, Siberia (Frantsesson, 1970); Open hexagons = Cane Valley diatreme and Moses Rock dikes, Utah (McGetchin et al., 1973); Open diamond = chlorite inclusion in diamond (Mitchell and Gardini, 1977).

extraneous streaks from other incoherently oriented phase(s) also are present. Powder patterns of the bulk sample confirmed the presence of Ia and IIb materials. The Ia material in this specimen has a 2-layer sequence labeled "t" by Mathieson and Walker (1954). They found this sequence in a vermiculite from Kenya, which they believed to be the average result of the equal probability of adoption of the 2-layer sequences "q" and "r". In both of these structures adjacent layers are related by 120° rotations, but differ in the sense of the $b/3$ shifts. De la Calle et al. (1976) and De la Calle et al. (1978) determined experimentally that the vermiculite "t" structure (V_{II} in their terminology) transforms only to phlogopite- $2M_1$, which also incorporates 120° layer rotations in its structure and is considered the parent material. Both

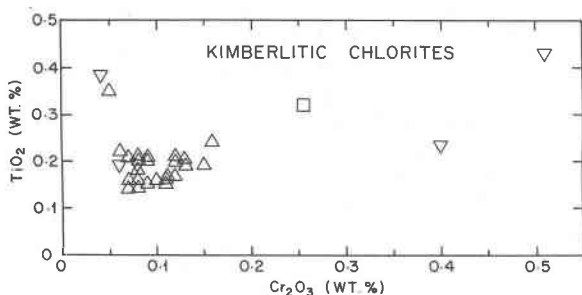


Fig. 5. Chemical variation plot from individual Koidu chlorite analyses (apex up triangles). Only the groundmass chlorites have been distinguished as shown by apex down triangles. Square = Mir pipe, Siberia (Frantsesson, 1970).

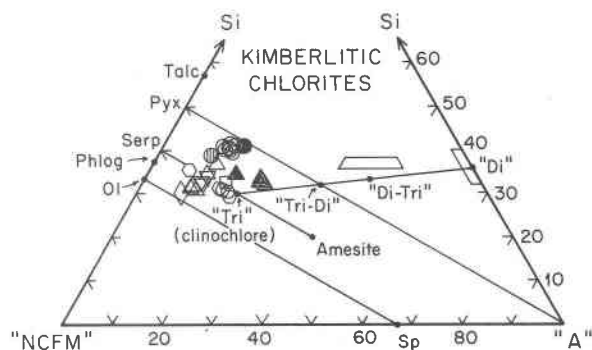


Fig. 6. A ternary diagram summarizing all data on kimberlitic chlorites presented in this paper. The compositional plotting scheme is adopted from Robinson et al. (1982) in which "NCFM" = $Fe^{2+} + Mg + Mn + Ca + 2Na + 2K - Ti$, and "A" = $Al + Fe^{3+} + Cr + 2Ti - Na - K$. Areas outlined represent natural occurring Di-Tri and Di-octahedral chlorites as summarized by Eggleton and Bailey (1967). Pyx = pyroxene, Serp = serpentine; Phlog = phlogopite; Ol = olivine; Sp = spinel. Symbols are the same as in Figure 4. See text for further explanation.

phlogopite- $2M_1$ and vermiculite "t" = V_{II} are rare in nature. De la Calle et al. (1976) and De la Calle et al. (1978) conclude from the modulated streaks along the 02l row line that V_{II} also is a semi-ordered structure in which there is an equal probability of a $+b/3$ or a $-b/3$ shift of a given layer. Instead of describing it as an average structure of the regular "q" and "r" sequences, therefore, V_{II} is better described as semi-ordered with a layer sequence given by $+120^\circ \pm b/3, -120^\circ \pm b/3, +120^\circ \pm b/3$, etc. It is

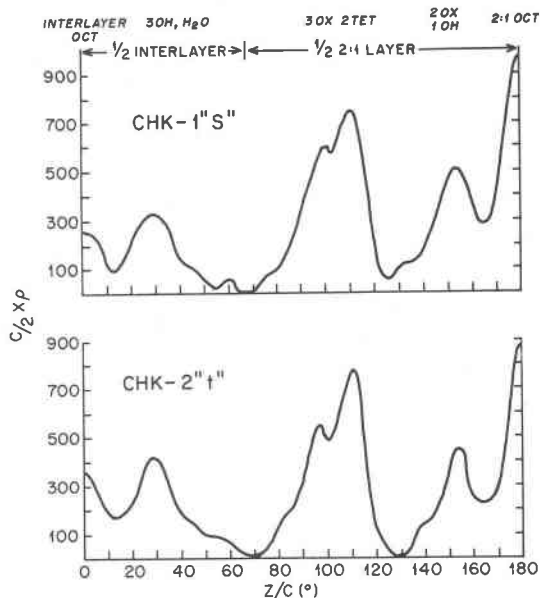


Fig. 7. One dimensional electron density projections for chlorite samples CHK-1 and CHK-2.

not known in specimen CHK-2 whether or not the Ia stacking sequence is restricted to the collapsible vermiculitic layers and the Iib sequence to the chloritic layers, but this is a possibility.

Plates from specimen CHK-13 readily break into fibers upon cutting. Six fibers were found to give superposition of Ia and Iib chlorite patterns on precession photographs. This overlap prevented determination of the precise stacking sequence of layers in each phase. The Iib chlorite is the most abundant structural type and is believed by Bailey and Brown (1962) to be the most stable chlorite. It is the only chlorite to be synthesized to date, and is the only chlorite structural type found in the greenschist metamorphic facies, except in clearly retrograde reactions. Thus it is considered the higher temperature form of chlorite, somewhat analogous to the *1M* polytype in the phlogopite system and the *2M₁* polytype in the muscovite system. It is not known whether or not the Ia stacking sequence is restricted to the collapsible layers in specimen CHK-13.

Discussion

Experimental studies on the alteration of phlogopite to vermiculite, or vice-versa, (De la Calle et al., 1976; De La Calle et al., 1978) show without exception that 2-layer type *V_I* ("s") structures form from *1M* phlogopites, and that type *V_{II}* ("t") structures result from *2M₁* phlogopites. Neither of these 2-layer structures has been recognized previously in chlorite and may be restricted to the vermiculite phases. Soboleva et al. (1982) studied phlogopites from the Yakutian kimberlites and determined that all specimens they examined are *1M* polytypes. These data coupled with the selective replacement of early macrocrystic phlogopites by chlorite at Koidu suggests that the precursor phase to the discrete chlorite nodules was probably phlogopite and that the ultimate end product would be vermiculite. This sequence of kimberlite pre and post emplacement alteration (phlogopite–chlorite–vermiculite) is consistent with that proposed by Kreston (1973).

The phlogopite (R)–chlorite macrocrysts lend strong support in favor of a similar phlogopite composition for the discrete nodules; some xenocryst-like chlorites in the groundmass may represent disaggregated nodules. Identical Cr_2O_3 and TiO_2 contents between the chlorite nodules and core phlogopites (R) are observed (Tompkins, 1983). Such low Cr_2O_3 , TiO_2 , and Al_2O_3 values represent growth in a highly depleted environment. Deformation kink bands in the nodules (Fig. 2) and chemical homogeneity of the core (R) phlogopites (Tompkins and Haggerty, 1983a) is compatible with crystal growth in a mantle source region prior to incorporation in the kimberlite host (Boyd and Nixon, 1978; Farmer and Boettcher, 1981).

Experimental studies on the oxidation state of Fe in potassium rich melts show that Fe is dominantly in the trivalent state, and that Fe^{3+} behaves as a tetrahedral

species in peralkaline conditions (Dickenson and Hess, 1981). Potassium will act as an efficient charge balancing species and tetrahedral Al^{3+} expands the framework to allow the substitution of Fe^{3+} in the tetrahedral site. The early core phlogopites (R) are reversely pleochroic, most probably due to the effects of tetrahedral Fe; they represent crystallization from a depleted potassium-rich source in which tetrahedral Fe^{3+} played an important role in the absence of sufficient Al^{3+} . Late stage reactions of disseminated early phlogopite nodules with the kimberlite liquid has permitted the nucleation and growth of Ti and Cr enriched phlogopites.

Forbes and Flower (1974) have demonstrated experimentally that Ti-rich phlogopites are more stable under mantle conditions than Ti-free phlogopites. If Ti acts as a stabilizer to the phlogopite structure then the preferential replacement of the reversely pleochroic phlogopites by chlorite may result from Ti depletion and Fe enrichment. The other possibility is that chlorite replacement occurred during a "chlorite event" as the rising kimberlite magma passed through the chlorite stability field. Late stage precipitation of Ti-rich groundmass phlogopite unaltered by, and in conjunction with chlorite (Fig. 3) further emphasizes the stabilizing effect of Ti on phlogopite and the probable primary occurrence of groundmass chlorite.

Water– CO_2 activity appears to be the driving mechanism for chloritization in the kimberlite. Vermiculite is present only in weathered kimberlite (Fairbain and Robertson; 1966) under hydrous and post emplacement conditions. When CO_2 activity is low, phlogopite (R+N) is more stable and chlorite is present in minor amounts. Some core phlogopites may even remain totally unaffected by chloritization. As phlogopite becomes unstable under conditions of increasing carbonitization, the reaction to chlorite requires the formation of brucite and the release of interlayer K. Magnesium ions must, therefore, be in abundance and readily available for linkage with hydroxyl molecules. In the carbonatitic kimberlites, olivine is pseudomorphed by calcite, and chlorite is stable relative to phlogopite (Tompkins and Haggerty, 1983b). The carbonitization of olivine is, hence, a probable source to produce the required flux of Mg ions required for brucite formation. The $X_{\text{H}_2\text{O}}/X_{\text{CO}_2}$ ratio or changes in *P–T* conditions would be required to decrease sufficiently, subsequent to carbonitization, to permit the formation of brucite and the ultimate demise of phlogopite. This is necessary because positively charged brucite layers replace the interlayer K ions. Highly mobile K ions can be more readily transported in volatile rich fluids and may precipitate to form other late-stage K-bearing phases. Erlank and Rickard (1977) and Erlank et al. (1982) consider K-metasomatism to be widespread in the upper mantle and although we have no direct evidence that K-mobilization is related to the processes we invoke, the removal of K is nonetheless required for the transformation of phlogopite to chlorite. It is possible that the high K-chlorites

contain a vestige of earlier phlogopite and in this sense represents incipient transformation to chlorite and/or vermiculite. Primary, euhedral groundmass chlorite is Fe-enriched and these are comparable in most respects to the most Fe-rich chlorite nodules.

The formation of phlogopite was at lower P - T conditions than the diamond/graphite transition in the depleted portion of the peridotite mantle (Farmer and Boettcher, 1981). Phlogopite intergrowths with diamond (Prinz et al., 1975) are typically very high in TiO_2 (10.8 wt.%) consistent with growth from an evolved liquid. MARID suite rocks (which are most similar to the core phlogopite (R) in composition) are considered to have equilibrated under relatively shallow depths resulting from early plutonic kimberlite pulses (Dawson and Smith, 1977). In the system $\text{MgO-SiO}_2\text{-CO}_2\text{-H}_2\text{O}$ the subsolidus formation of brucite and carbonate from forsterite and vapor occurs with decreasing temperature and/or increasing pressure and $\text{H}_2\text{O/CO}_2$ values (Ellis and Wyllie, 1980). Based on the stability of K-richterite (Kushiro and Erlank, 1970), the MARID suite nodules are considered to have crystallized at depths of 75–100 km. At these depths the chlorite dehydration reaction curve (Jenkins, 1981) intersects the Precambrian shield geotherm and is also coincident with the depth where CO_2 ceases to be a dominant solidus component (Wyllie, 1980), implying that high fluxes of CO_2 vapor are present.

Experimental and theoretical studies of the Mg end-member clinocllore (Jenkins, 1981; Obata and Thompson, 1981) show that chlorite (type IIb) can be stable at low temperatures (<900°C) up to ≈ 75 km in the upper mantle and an alternative possibility is that some of the Koidu chlorites (types Ia, and Ia/IIb) are not pseudomorphs after phlogopite. Chlorite in diamond inclusions (type Ib; Mitchell and Giardini, 1977) are similar to our low Fe chlorite compositional type in FeO, SiO_2 , and Al_2O_3 contents only. In the two inclusions reported, one is exceptionally enriched in CaO (10.7 wt.%) and probably represents an overlap with coexisting clinopyroxene, the other is a high magnesian variety (40.3 wt.%) with almost twice the concentration of MgO than those from Koidu. Although, the most stable chlorite polytype is type IIb it is interesting to note that the diamond inclusion is not a IIb but type Ib. Whether type Ia chlorites are stable at mantle P and T 's under appropriate conditions is uncertain. Given these uncertainties it is still possible that the Koidu chlorite nodules are indeed primary upper mantle phases. The experimental data are not entirely appropriate to the compositions we discuss and data are clearly required to evaluate the high pressure stability of low Al_2O_3 , high Mg-Fe chlorites.

Conclusions

Chlorite is present in three modes of occurrence in the Koidu kimberlite complex: (1) discrete nodules with fibrous, platy, tectonized, or multiply cleaved textural

habits; (2) coarse anhedral macrocrysts and small euhedral platelets in kimberlite groundmass; and (3) as preferential replacement products of reversely pleochroic phlogopite. The chlorites are compositionally distinctive, high in SiO_2 and MgO and low in Al_2O_3 contents. Three dominant compositional types are designated as high (25 wt.% FeO), intermediate (15 wt.%) and low (8 wt.%) FeO varieties, with a minor type that is low in iron but high in K_2O . Compositions, comparisons with ideal chlorite, and electron density measurements, suggest extensive vacancies in the interlayer sheet. Fibrous specimens are Ia structural types, ubiquitous in vermiculite but among the least abundant of the chlorites found in nature. There is evidence for nearly complete transformation to vermiculite and for phlogopite as a precursor. Platy chlorites are intergrown Ia and IIb structural types, the latter being of relatively high temperature origin, the most stable among chlorites, and the most abundant structural type in nature.

Euhedral kimberlite groundmass chlorites are unequivocally of primary magmatic origin and high TiO_2 contents are consistent with crystallization from a residual melt. Carbonatite associations or high calcite contents, and the alteration of phlogopite to Ia chlorite implies chloritization under high X_{CO_2} activity. This condition prevailed in a volumetrically minor component of Pipe 2 and in many of the kimberlite dikes, suggesting that CO_2 volatilization was impaired, possibly because these facies were passive intrusions. By contrast, the dominant diatreme facies were explosive and enriched in H_2O , and this resulted in serpentine + phlogopite. Although eclogites are the only lithic nodules identified at Koidu that can be directly linked to a fertile asthenosphere, it is also possible that metasomatized lithosphere was sampled in the form of phlogopite nodules that are now completely transformed to chlorite.

The chlorites we describe may not be of mantle origin; additional chemical and crystallographic data are required on these and chlorites in other kimberlites. Experimental data appropriate to these compositions are also needed to determine the conditions required for Ia and IIb type chlorite formation, and to address the problem of chlorite stability in the upper mantle.

Acknowledgments

This research was partially supported by National Science Foundation grants EAR 78-02539, EAR83-08297 (to S.E.H.), and EAR-8106124 (to S.W.B.). Access to, and logistical support at the Koidu kimberlite complex was made possible by B.P. Minerals and Sierra Leone Selection Trust. Management and geological staff are thanked for their help in obtaining critical samples in this and the overall project. Peter Robinson has had a continued interest in the chlorite problem and is thanked for fruitful discussions. D. Leonard was responsible for maintaining the electron microbeam facility and D. Volz aided in the wet chemistry. Critical reviews and constructive comments were

provided by D. Hewitt and S. Bohlen. To all we express our gratitude.

References

- Albee, A. L. (1962) Relationships between the mineral association, chemical composition and physical properties of the chlorite series. *American Mineralogist*, 47, 851–870.
- Albee, A. L. and Ray, L. (1970) Correction factors for electron probe microanalysis of silicates, oxides, carbonates, phosphates, and sulfates. *Analytical Chemistry*, 42, 1408–1414.
- Bailey, S. W. (1980) Summary of recommendations of AIPEA nomenclature committee on clay minerals. *American Mineralogist*, 65, 1–7.
- Bailey, S. W. and Brown, B. E. (1962) Chlorite polytypism: I. Regular and semi-random one-layer structures. *American Mineralogist*, 47, 819–850.
- Bardet, M. G. (1974) *Geologie du diamant. Memoires du B.R.G.M., n°83, tome I and II.*
- Bence, A. E. and Albee, A. L. (1968) Empirical correction factors for the electron microanalysis of silicates and oxides. *Journal of Geology*, 76, 382–403.
- Boyd, F. R. and Nixon, P. H. (1978) Ultramafic nodules from the Kimberley pipes, South Africa. *Geochimica et Cosmochimica Acta*, 42, 1367–1382.
- Dawson, J. B. and Smith, J. V. (1977) The MARID (mica-amphibole–rutile–ilmenite–diopside) suite of xenoliths in kimberlite. *Geochimica et Cosmochimica Acta*, 41, 309–323.
- De la Calle, C., Dubernat, J., Suquet, H., Pezerat, H., Gaultier, J., and Mamy, J. (1976) Crystal structure of two-layer Mg-vermiculites and Na, Ca-vermiculites. In S. W. Bailey, Ed., *Proceedings of the International Clay Conference*, p. 201–209. Applied Publishing Ltd., Illinois.
- De la Calle, C., Suquet, H., Dubernat, J. and Pezerat, H. (1978) Mode d'empilement des feuillets dans les vermiculites hydratées a 'deux couches'. *Clay Minerals*, 13, 275–297.
- Dickenson, M. P. and Hess, P. C. (1981) Redox equilibria and the structural role of iron in aluminosilicate melts. *Contributions to Mineralogy and Petrology*, 78, 352–357.
- Eggleton, R. A. and Bailey, S. W. (1967) Structural aspects of dioctahedral chlorite. *American Mineralogist*, 52, 673–689.
- Ellis, D. E. and Wyllie, P. J. (1980) Phase relations and their petrological implications in the system $MgO-SiO_2-H_2O-CO_2$ at pressures up to 100 kb. *American Mineralogist*, 65, 540–556.
- Erlank, A. J., Alsopp, H. J., Hawkesworth, C. J., and Menzies, M. A. (1982) Chemical and isotopic characterization of upper mantle metasomatism in peridotite nodules from Bultfontein. *Terra Cognita*, 2, 261–263.
- Erlank, A. J. and Rickard, R. S. (1977) Potassium richterite bearing peridotites from kimberlite and the evidence they provide for upper mantle metasomatism. *Abs. Vol., Second International Kimberlite Conference*, Santa Fe, New Mexico.
- Fairbairn, P. E. and Robertson, R. H. S. (1966) Stages in the tropical weathering of kimberlite. *Clay Minerals*, 6, 351–370.
- Farmer, G. L. and Boettcher, A. L. (1981) Petrological and crystal-chemical significance of some deep-seated phlogopites. *American Mineralogist*, 66, 1154–1163.
- Fawcett, J. J. (1965) Alteration products of olivine and pyroxene in basalt lavas from the Isle of Mull. *Mineralogical Magazine*, 35, 55–68.
- Ferguson, J., Danchin, R. V., and Nixon, P. H. (1973) Fentization associated with kimberlite magmas. In P. H. Nixon, Ed., *Lesotho Kimberlites*, p.207–213. Lesotho National Development Corporation, Maseru.
- Fieremans, M. and Ottenburgs, R. (1979) Kimberlite inclusions and chlorite nodules from the kimberlite-breccia of Mbuji-Mayi (Eastern Kasai) Zaire. *Societe Belge de Geologie. Bulletin/ Belgische Vereniging Voor Geologie*, 88, 205–224.
- Flanagan, F. J., Ed. (1976) Descriptions and analyses of eight new USGS rock standards. Geological Survey professional paper 840, 192 pages.
- Forbes, W. C. and Flower, M. F. J. (1974) Phase relations of titan phlogopite $K_2Mg_4TiAl_2Si_6O_{20}(OH)_4$ a refractory phase in the upper mantle? *Earth and Planetary Science Letters*, 22, 60–66.
- Foster, M. D. (1962) Interpretation of the composition and a classification of the chlorites. Geological Survey professional paper 14 A.
- Frantsesson, E. V. (1970) The petrology of kimberlites. Translated by D.A. Brown, Department of Geology Publication No. 150, Australian National University, Canberra.
- Giardini, A. A., Hurst, V. J., Melton, C. E. and Stormer, Jr., J. C. (1974) Biotite as a primary inclusion in diamond: Its nature and significance. *American Mineralogist*, 59, 783–789.
- Grantham, D. R. and Allen, J. B. (1960) Kimberlites in Sierra Leone. *Overseas Geology and Mineral Resources. The Quarterly Bulletin of the Overseas Geological Survey, London*, 8, 5–25.
- Hall, P. K. (1970) The diamond fields of Sierra Leone. Geological Survey of Sierra Leone.
- Hayes, J. B. (1970) Polytypism of chlorite in sedimentary rocks. *Clays and Clay minerals*, 18, 285–306.
- Jenkins, D. M. (1981) Experimental phase relations of hydrous peridotites modelled in the system $H_2O-CaO-MgO-Al_2O_3-SiO_2$. *Contributions to Mineralogy and Petrology*, 77, 166–176.
- Kreston, P. (1973) Differential thermal analysis of kimberlites. In P.H. Nixon, Ed. *Lesotho kimberlites*, p. 269–279. Lesotho National Development Corporation, Maseru.
- Kushiro, I. and Erlank, A. J. (1970) Stability of potassic richterite. Annual report of the Director of the Geophysical Laboratory, Carnegie Institution of Washington Year Book, 68, 231–233.
- Lehmann, E. (1965) Non-metasomatic chlorite in igneous rocks. *Geological Magazine*, 102, 24–35.
- Mathieson, A. McL. and Walker, G. F. (1954) Crystal structure of magnesium-vermiculite. *American Mineralogist*, 39, 231–255.
- Maxwell, J. A. (1968) *Rock and Mineral Analysis. Chemical Analysis*, 27, 419.
- McGetchin, T. R., Nikhanj, Y. S. and Chodos, A. A. (1973) Carbonatite–kimberlite relations in the Cane Valley Diatreme, San Juan County, Utah. *Journal of Geophysical Research*, 78, 1854–1869.
- Mitchell, R. S. and Giardini, A. A. (1977) Some mineral inclusions from African and Brazilian diamonds: their nature and significance. *American Mineralogist*, 62, 756–762.
- Nixon, P. H. and Kreston, P. (1973) Butha-Buthe dyke swarm and associated kimberlite blows. In P.H. Nixon, Ed. *Lesotho Kimberlites*, p.197–206. Lesotho National Development Corporation, Maseru.
- Obata, M. and Thompson, A. B. (1981) Amphibole and chlorite in mafic and ultramafic rocks in the lower crust and upper mantle, A theoretical approach. *Contributions to Mineralogy and Petrology*, 77, 74–81.

- Pauling, L. (1930) The structure of the chlorites. *Proceedings of the National Academy of Science*, 16, 578–582.
- Prinz, M., Manson, D. V., Hlava, P. F. and Keil, K. (1975) Inclusions in diamonds: garnet lherzolite and eclogite assemblages. In L.H. Ahrens et al., Eds., *Physics and Chemistry of the Earth*, 9, 797–816.
- Robinson, P., Spear, F. S., Schumacher, J. C., Laird, J., Klein, C., Evans, B. W. and Doolan, B. L. (1982) Phase relations of metamorphic amphiboles: natural occurrence and theory. In D. R. Veblen and P. H. Ribbe, Eds., *Amphiboles: Petrology and experimental phase relations*, 9B, p. 1–228. *Reviews in Mineralogy*, Mineralogical Society of America, Washington, D.C.
- Schreyer, W. and Yoder, H. S., Jr. (1964) The system Mg-cordierite–H₂O and related rocks. *Neues Jahrbuch für Mineralogie, Monatshefte*, 101, 271–342.
- Shirozu, H. and Bailey, S. W. (1965) Chlorite polytypism III: Crystal structure of an orthohexagonal iron chlorite. *American Mineralogist*, 50, 868–885.
- Shirozu, H. and Bailey, S. W. (1966) Crystal structure of a two-layer Mg-vermiculite. *American Mineralogist*, 51, 1124–1143.
- Sobolev, N. V. (1977) Deep-seated inclusions in kimberlites and the problem of the composition of the upper mantle. American Geophysical Union, Washington, D.C.
- Soboleva, S. V., Khar'kiv, A. D., Zinchuk, N. N. and Kotel'nikov, D. D. (1982) Characteristics of phlogopite of mantle origin. *International Geology Review*, 24, 35.
- Tompkins, L. A. (1983) The Koidu Kimberlite Complex, Sierra Leone, West Africa. M.S. thesis, University of Massachusetts.
- Tompkins, L. A. and Haggerty, S. E. (1983a) The Koidu kimberlite complex, Sierra Leone: Geological setting, petrology, and mineral chemistry. *Proceedings of the third International Kimberlite Conference, Developments in Petrology*, Volume I, Elsevier Pub. Co., in press.
- Tompkins, L. A. and Haggerty, S. E. (1983b) The Koidu kimberlite complex, Sierra Leone: Geological setting, petrology, and mineral chemistry: appendix. IIIeme conf. int. kimberlites, "Documents," J. Kornprobst ed., Ann. Univ. Clermont Fd., in press.
- Wyllie, P. J. (1980) The origin of kimberlite. *Journal of Geophysical Research*, 85, 6902–6910.

*Manuscript received, February 21, 1983;
accepted for publication, October 3, 1983.*